APPLICATION OF A NEW HYBRID MATERIAL (ARALL)
IN AIRCRAFT STRUCTURES

J.W. Gunnink, L.B. Vogelesang and J. Schijve

Delft University of Technology
Department of Aerospace Engineering
Delft - The Netherlands

ABSTRACT

A new material for aircraft structures with several promising properties is described. The material is obtained by the adhesive bonding of a number of thin aluminium alloy sheets and aramid layers to produce an aramid reinforced aluminium laminate (ARALL).

ARALL shows very favourable fatigue crack growth properties and has a high tensile yield strength. This is especially true if suitable residual stresses are introduced into a laminate with an optimum thickness of metal sheets. Comparative tensile and fatigue tests have been carried out on notched and centrally cracked specimens, bolted and riveted joints and lugs of ARALL, with tests on monolitic material as reference. The results of buckling tests are compared with corresponding calculations for both aluminium alloy and ARALL compression panels.

Design calculations on pressure cabins representative of various current aircraft show the possible weight savings to be obtained in this application.

Some design considerations for the general use of ARALL in aircraft structures are presented.

INTRODUCTION

An important step towards the further development of laminated sheet material is the addition of "high modulus" fibres into the bondline. Previous investigations had already indicated a potential gain in fatigue crack growth resistance. However, it will be shown that a completely new hybrid material, with superior properties, can be obtained by:
- optimization of the amount of fibres and fibre orientation in relation to the thickness and the type of alloy of the metal sheets;
- prestressing of the fibres during curing to introduce a favourable residual stress system in the fibres (in tension) and the sheet (in compression).

Starting from these considerations a new materal was developed at the Department of Aerospace Engineering of the Delft University of Technology. This material is called ARALL: aramide reinforced aluminium laminate. Application of ARALL in aircraft structures can lead to large weight savings, especially where fatigue and damage tolerance are important design criteria. Well-known examples are wing tension skins, and pressure cabins of transport aircraft.

In the present paper the following topics will be discussed.
1. First, basic considerations and the development of ARALL will be reviewed, including the introduction of a residual stress system.
2. Various properties of ARALL will be summarized, not only material properties but also production aspects.
3. A design excercise of a wing structure indicated

that application of ARALL could lead to considerable weight savings. To provide data for this application several series of tests were carried out, and the results will be presented.
4. The excercise also indicated that panel buckling, due to negative gusts, may become the design case even for the tension skin of the wing, if fatigue is no longer critical. A new computer program for buckling was developed for this purpose, and calculations are compared with test results.
5. Finally, possible weight savings for pressure cabins designed in ARALL are examined.

ARALL MATERIAL, BASIC CONSIDERATIONS AND PRODUCTION ASPECTS

ARALL is built up as laminated sheet material, preferably of a high strength aluminium alloy, with uni-directional fibre reinforcements in the bond layers[1]. A cross-section is shown in Figure 1. The excellent fatigue properties are obtained primarily by restraint on fatigue crack opening as a result of the presence of uncracked fibres (Figure 2). Tests have already shown that this mechanism is effective for very small cracks (of the order of a few millimeters). Fatigue cracks grow under cyclic tensile stress in a direction perpendicular to the maximum principal stress. For this reason unidirectional fibres should be orientated in the direction of the maximum principal stress. In this way ARALL combines the favourable properties of high strength aluminium alloy with the good anisotropic fatigue resistance of fibre reinforced materials.

The main variables in optimising the material itself are:
1. The sheet material, i.e. type of alloy and sheet thickness.
2. The type of fibres.
3. The adhesive bonding system.
4. The residual stress system.
Each of these points will now be explained further.

Point 1. Initially laminates were made from 2024-T3 alclad sheet, but it was already evident at that time that internal cladding layers have no purpose. Bare sheet material would be preferred, also because of the possibility of bond line corrosion. Moreover, 7075-T6 is a better choice than 2024-T3 in view of its higher yield stress. The poor fatigue resistance of 7075-T6 is fully compensated by the excellent fatigue behaviour of ARALL. With regard to the thickness of the individual metal sheet a small sheet thickness is desirable ($\leq$ 0.5 mm). More thin sheets to build up a certain total thickness implies more adhesive layers. As a result the interlaminar shear flow between unbroken fibres and fatigue crack edges will be lower. This implies a limited delamination and more effective crack opening restraint.

Point 2. Aramid fibres have been chosen instead of the better known carbon fibres for the following reasons:

1. Aramid is electrically neutral relative to metals. Galvanic corrosion problems are not expected.
2. Higher specific strength and higher failure strain in tension than carbon fibre.
3. Less expensive.
A disadvantage of aramid fibres is their low compressive strain to failure. In spite of this, the compressive strength of ARALL is good, due to the favourable residual stress system, as will be discussed later.

Point 3. Adhesive properties required are:
1. Good adhesion to anodized aluminium surfaces and to aramid fibres.
2. Non-brittle after curing.
3. Low specific weight
4. Good durability.
The significance of good fibre and adhesive properties is readily understood in view of the crack opening restraint to be exerted by the fibres and transmitted through the adhesive to the sheets.

Point 4. The amount of prestressing of the fibres during curing determines the residual stress system within the ARALL material after curing. It has a major effect on the fatigue and compressive properties.

Production aspects

Two types of ARALL material have been investigated:

Type A: ARALL built up from thin 2024-T3 or 7075-T6 bare sheets and single aramid Kevlar-143 fabric layers bonded together with BSL 312-UL adhesive (Figure 1). The 143 weave is not fully unidirectional: 90% of the fibres are in the longitudinal direction and 10% in the transverse direction (fibre volume content 40%).

Type B: Superior to type A and built up from thin 2024-T3 or 7075-T6 bare sheets and single unidirectional ARENKA AF 163-2 "prepreg" layers (fibre volume content 55%) (Figure 3).

Prior to assembly the aluminium sheets are pretreated as follows: alkaline degreased; pickled in chromic-sulphuric acid; chromic acid anodized and primed with BR127, which is a modified epoxy phenotic primer with corrosion inhibiting properties.

The curing is performed in an autoclave for 30 minutes (BSL312) or 60 minutes (AF 163-2) at a temperature of 120° C. The pressure during curing was held at 6×10^5 Pa (6 bar).

As a result of the different thermal expansion coefficients of aluminium alloy (α_{Al}) and the aramid fibre layer (α_{Ar}) residual thermal stresses are present after cooling down from the curing temperature (T_0) to a lower temperature (T). The residual stress in the aluminium alloy sheet follows from Reference 2:

$$(S_i)_{Al} = E_{Al} \left(1 + \frac{t_{Al} E_{Al}}{t_{Ar} E_{Ar}}\right)^{-1} (\alpha_{Al} - \alpha_{Ar}) \times$$
$$\times (T_0 - T) \qquad (1)$$

In this equation t_{Al} is the total thickness of the aluminium sheets and t_{Ar} the total thickness of the adhesive bond layers with aramid fibres. The corresponding elastic moduli are E_{Al} and E_{Ar}. It should be kept in mind that α_{Ar}, t_{Ar} and E_{Ar} are associated with a bond layer containing aramid fibres. These quantities will therefore depend on the fibre volume percentage. For the undirectional

prepreg, measurements indicate $\alpha_{Ar} = 5.7 \times 10^{-6}$, which is smaller than $\alpha_{Al} = 23 \times 10^{-6}$. According to Equation (1) a tensile residual stress will occur in the aluminium alloy sheets and as a consequence the residual thermal stress in the aramid fibres will be compressive. The curing cycle evidently produces an unfavourable residual stress distribution.

Fortunately it is possible to reverse the sign of the residual stresses obtained after curing. Until now this has been done by prestraining the ARALL after curing, until some small plastic strain is produced in the metal sheets. The result obtained is illustrated in Figure 4, where the load-strain curves of the aluminium alloy sheets and the aramid layers are shown separately. Prestraining up to points A, B, C in Figure 4 (B in the plastic range of the sheets), followed by unloading leads to a reverse of the signs of the residual forces. This kind of ARALL material will be referred to as prestrained ARALL. After prestraining the fibres are now in tension, causing the metal sheets to be in compression. The fatigue properties, already good even without prestraining, are improved further. A disadvantage of prestraining is a lower yield stress in compression (the Bauschinger effect). To avoid this phenomenon a better method of obtaining a favourable residual stress system is to cure the material with the fibres under tension. This kind of ARALL material will be referred to as prestressed ARALL. Some pilot experiments have shown that this is a feasible technique and a proportional limit in compression of 400 MPa was obtained[3].

PROPERTIES OF ARALL

Specific weight
In view of the presence of adhesive and aramid fibres the specific weight is more than 14% lower than for aluminium (see table below).

Static properties
The yield stress and the ultimate tensile strength of ARALL are higher than for the aluminium alloy of which it is composed. Also notched ARALL is stronger, while the same has been found for different kinds of bolted and riveted joints. However, the failure strain is comparatively low, due to the failure strain of the fibres. For a fatigue sensitive material this could be disastrous, but for ARALL it is not, as will be shown by the experimental data. ARALL could be used to replace aluminium alloy 2024-T3 in aircraft structures. The table below gives an impression of the advantage that could be obtained.

	2024-T3*	7075-T6*	ARALL
0.2% yield stress [MPa]	360	480	500
ultimate tensile stress [MPa]	470	560	700
proportional limit in compression [MPa]	270	480	400
blunt notch strength** [MPa]	450	530	550
specific weight	2.8	2.8	2.45

* non-clad
** hole notched specimen, $K_t = 2.43$, strength based on net section.

Fatigue properties
These are discussed later.

Corrosion behaviour
An extensive program has been started to investigate the corrosion behaviour of ARALL. This program includes corrosion tests on I.L.S. (interlaminar shear), Bell peel, wedge edge and delamination specimens in different environments. Also the influence of temperature and humidity and the effect of static and dynamic loading on corrosion behaviour is being investigated. Results available sofar are encouraging and indicate that durability problems are not to be expected. In general, certification of structures in ARALL should not meet with significant difficulty in view of the present experience in adhesive bonding technology (successfully applied in many Fokker designs as witnessed by 25 years of experience with the Fokker F27 Friendship).

Relaxation of residual stress
Creep in the aramid fibre could imply a relaxation of the residual stress system. However, from what is known about aramid fibre, this is not to be expected. A program to measure the residual stress over long periods on specimens under tensile load and different temperatures has been started. Preliminary results indicate that relaxation does not occur.

A second adhesive bonding treatment of ARALL sheets (involving pretreatments and high temperature curing) was applied. No degradation of properties and no relaxation of residual stress could be observed.

Cutting and sheet forming
For the preparation of specimens it was necessary to saw the material to the rough dimensions, followed by contour milling and drilling of holes. All these operations were easily done by normal workshop procedure. Tests have also proved that countersinking is possible.

Plastic bending of ARALL requires some special attention, in view of the limited failure strain of the aramid fibres and the possibility of delamination due to the high shear stresses involved in bending. For the production of stringers these restrictions should not be serious, because the fibres are in the longitudinal direction, whereas bending occurs in the transverse direction. An extensive program to determine the limitations and the best bending technique for ARALL, is just now reaching success with the manufacture of Z- and hat-stiffeners (Figure 5).

STRUCTURAL DEVELOPMENT PROGRAM FOR A TRANSPORT AIRCRAFT WING

Because ARALL is highly fatigue-insensitive it should find its main benefits in fatigue sensitive areas of aircraft structures such as the lower wing skin of a transport aircraft and the skin of a pressure cabin. In order to evaluate the advantages and to explore problem areas it was decided to re-design the lower wing skin of the outer wing of the Fokker F27 Friendship. A structural development program was set up for this purpose to be completed by manufacturing and testing a full-scale part of the structure in ARALL, as indicated in Figure 6. To achieve a realistic comparison with the existing structure the lower skin of the outer wing has to be redesigned in ARALL for all the same design loading cases. The F27 wing was selected because full information on design loads, structural lay-out, dimensions and weight of the existing structure was available. Moreover the F27 wing panel indicated in Figure 6 has been tested extensively by Fokker[4].

An initial design of the lower skin of the outer wing in ARALL has shown a weight saving of 30%[5]. The design study also indicated that the "negative gust" case now becomes the critical design case. This is a consequence of the fatigue-insensitivity of ARALL on the one hand and the gust sensitivity of small transport aircraft on the other hand. So the compression characteristics of ARALL and the buckling behaviour of ARALL stiffened skin panels becomes important. Therefore the structural development program includes buckling tests as well as an analytical study, which has led to a new calculation method. The program is well in progress, but not yet completed. Significant results available are described below.

Fatigue test results
Tests were carried out with flight-simulation loading (standardized TWIST load sequence) and with constant-amplitude loading. The results of five series of tests are mentioned below:

1. Flight-simulation tests have been carried out on monolithic material, on laminated material (without fibres) and on ARALL. The results in Figure 7 for crack growth up to failure show that the laminated material is already considerably better than monolithic material. However, ARALL shows a further significant improvement, even for unprestrained ARALL. After prestraining and increasing the stress level (mean stress in flight S_{mf} = 100 MPa) no fatigue failure could be obtained. As a result of uncracked fibres in the wake of the crack and the residual stresses due to prestraining the stress intensity factor is drastically reduced and almost complete crack arrest is obtained.

2. Constant-amplitude tests (see Figure 8) show a remarkable and characteristic behaviour of prestrained ARALL. After a very large number of cycles the aluminium sheets of a prestrained specimen are completely cracked, while the specimen as a whole still has the ability to transmit loads. Because of the uncracked fibres this results in a very long fatigue life.

3. Constant-amplitude tests were carried out on lug specimens made from monolithic, laminated and ARALL material with different metal sheet thicknesses (Figure 9). All specimens have the same aramid/aluminium ratio. The longest fatigue lives were found for the ARALL specimens. A larger increase in fatigue life was achieved by decreasing the layer thickness from 0.6 mm to 0.3 mm.

4. Flight-simulation tests (TWIST) under corrosion fatigue conditions on bolted joint specimens were perfomed within the framework of an AGARD-co-ordinated co-operative program[6]. Tests were carried out on ARALL and monolithic bolted joint specimens (using Hi-lok countersunk bolts) with a high load transfer (see Figure 10). The prestrained ARALL specimens did not fail in laboratory air in spite of extremely long test lives. Two test series were performed on pre-exposed specimens (72 hours in NaCl + SO_2). Pre-exposure was followed by fatigue in air in one test series and by fatigue in a salt spray cabinet in the other. No influence of pre-exposure was found for the ARALL specimens, contrary to the results for the monolithic specimens. In all prestrained ARALL specimens small

cracks did indicate, as revealed by undoing the un-
failed bolted joints. Apparently crack arrest
occurred in a similar way to the centre cracked
specimens.

The ARALL specimens also showed a behaviour
superior to the monolithic specimens in corrosion
fatigue (125000 compared to 5000 flights!). The
corrosion fatigue flight simulation tests were
carried out by the National Aerospace Laboratory
NLR.

5. Flight-simulation fatigue tests (TWIST) were
carried out on double butt strap and single butt
strap bolted joint specimens (Hi-lok bolts). The
fatigue life results in Figure 11 for different
S_{mf} values show again the superior behaviour of the
ARALL specimens compared with the monolithic speci-
mens[7].

Local Buckling

Local buckling behaviour was the first subject
of investigation for ARALL material in compression.
For this purpose hat-stiffeners were chosen for the
test specimens (see Figure 6). Both ARALL and
aluminium alloy hat-stiffeners were tested.

The dimensions of the cross-section are chosen
on the basis that all elements buckle more or less
simultaneously. The length of the hat-stiffener is
dictated by the calculated Euler-torsional buckling
strength.

A test specimen in the compression machine is
shown in Figure 12. The transducers w_r and w_ℓ at
the middle of the free flanges and w_m at the middle
of the top flange measure the out-of-plane dis-
placements of each element. The transducers u_ℓ and
u_r measure the shortening of the test specimen.

The results of a test run on an ARALL specimen
are given in Figures 13 and 14. In Figure 13 the
load P is plotted against shortening u, together
with the out-of-plane displacements w_m, w_r and w_ℓ.
In Figure 14 a view of the buckle pattern for the
test specimen is given, by means of scanner w_s.

Because prestraining of ARALL lowers the allow-
able compressive stress (Bauschinger effect in the
sheets) it was decided to use non-prestrained ARALL
for the test specimens.

The test results in Figure 13 show clearly the
point of fibre failure. The overall strain of the
test specimen at this point is $\varepsilon = -.31\%$. The
strain in the aramid layers due to the curing pro-
cess must be superimposed on the overall strain.
This strain is $\varepsilon_0 = -.16\%$ and so the total strain
in the aramid layers at fibre failure becomes
$\varepsilon_f = -.47\%$. This agrees very well with the data
given by the fibre manufacturers (Dupont and ENKA).

From the test results it follows that the com-
pressive Young's modulus of the aluminium alloy
test specimens is about 72000 MPa, which agrees
well with the widely used value, but the ARALL test
specimens have a compressive Young's modulus of
about 63000 MPa. This is not in agreement with the
predicted value of about 70000 MPa. It seems
necessary to investigate further the compressive
Young's modulus of (U.D.) aramid laminates, also
the compressive Young's modulus of ARALL itself.

Since fibre failure occurs before buckling,
local buckling calculations for the ARALL specimens
are performed without any contribution of the
fibres. This method of calculation agrees quite
well with the test results (see the table below).

For the ARALL designs, fibre failure occurs at
a stress of about -200 MPa. In practice this stress
will be much too low, especially if it is taken in-
to account that fibre failure destroys the good fa-
tigue properties. This, together with the inferior

fatigue behaviour of non-prestrained ARALL, is the
reason to look at an alternative method to pre-
stress ARALL. This alternative method is already
discussed. The next step will be to investigate the
local buckling behaviour of prestressed ARALL con-
figurations.

test specimen	$\dfrac{P_{calculated}}{P_{tested}}$
ARALL 1	1.02
ARALL 3	.92
Al 2	.94
Al 4	.98

Z-stiffened panels

The design study mentioned before shows that the
lower wing designed in ARALL actually becomes com-
pression, rather than tension, critical. In order
to make an effective design possible, it was
necessary to develop a computer program to cal-
culate the compression strength of orthotropic Z-
stiffened panels. So, in contrast to many of the
existing programs, this program has to accept
orthotropic as well as isotropic material proper-
ties. But more important perhaps, some design
variables are contained in the ARALL material it-
self, e.g. ratio of aluminium alloy to net ARALL
thickness and actual thickness of the individual
separate aluminium alloy sheets. Thus with this
program it should be possible to perform parametric
design studies in which both the material and the
panel design are considered at the time. Finally,
as an effective design tool, the program has to be
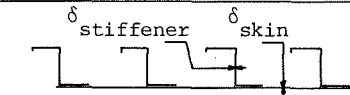very fast.

In 1980 Van der Neut published his method valid
for Z-stiffened panels made of isotropic linear
elastic material[10]. An extension of this method
is developed for panels composed of orthotropic
material[11]. A brief description of this (extended)
Van der Neut method will be given here, but for
detail information reference should be made to the
reports mentioned above.

A diagram of the particular buckling mode found
to be critical is shown in Figure 15. Because the
principal axes of the stiffeners are not parallel
and perpendicular to the plate, the overall buck-
ling mode is not a pure Euler mode. Overall buck-
ling can be regarded as an Euler mode accompanied
by sideways bending of the top flange of the
stiffener, thereby causing deformation of the cross-
section of the panel. Out-of-plane bending of the
web of the stiffener is restrained at the bottom of
the web by the plate and its bonded-on flange. The
stiffness of this restraint α is very important for
the resistance of the top flange to its deflection.
Deformation of the cross-section, together with the
shear flexibility causes a reduction k in the
Euler buckling load P_E. So the overall buckling
load is affected through the coefficient k in the
formula $P = k (\pi^2 D/L^2)$, whereby D is the bending
stiffness of the panel (section). However, the fac-
tor k is a function of the restraint coefficient α,
the number of half waves n and the shear buckling
coefficient k_s, where k_s is the ratio between the
buckling load at infinite bending stiffness P_s and
the Euler load P_E. A solution procedure to cal-
culate this coefficient k is given in Reference 11.

Sofar local buckling, often important in
stiffened panels, has not been incorporated in the
method described. This will be one of the main
points for further development. However, to make a

fast calculation and design possible the extended Van der Neut method is already programmed in the computer code OBSOZPAN (overall buckling of speically orthotropic Z-stiffened panels)[12]. In addition, because the buckling load of heavily loaded metal panels is strongly influenced by plasticity, a plasticity correction routine is incorporated in the program. This routine is based on the Ramberg-Osgood method.

Test results for aluminium alloy Z-stiffened panels with strong bond layers have shown that the calculated overall buckling loads are accurate to within a few percent, but it is also found that the calculated loads differ much more for the test panels with weak bond layers (see table below). So the influence of the bond layer can not be ignored. Van der Sloot has already discussed this phenomena [13] and makes clear that high stresses in the bond layer occur due to the buckling mode of the test panels. As the test panels have free unloaded longitudinal edges and a comparatively small width, the whole panel can rotate. This effect, as well as the lack of support for the stiffeners at the free edge, lowers the buckling load calculated with the program OBSOZPAN. However, this will not happen in the same way in real aircraft structures.

| | | 7075 aluminium alloy | |
| | | L = 1400 mm | |
panel code	bond type	$\dfrac{\delta_{stiffener}}{\delta_{skin}}$	$\dfrac{\bar{P}_{TEST}}{\bar{P}_{OBSOZPAN}*}$
PL-1	EC-2216 FM123-5	$\dfrac{2.3}{2.5}$	.84 .93
PL-2	EC-2216 FM123-5	$\dfrac{3.4}{4.1}$	.86 .93
PL-3	EC-2216 FM123-5	$\dfrac{4.0}{5.1}$	.80 .93

* without correction for the free longitudinal edges

Comparison between test results and computed results of aluminium Z-stiffened panels.

Tests on complete ARALL panels will be carried out shortly.

Some Z-section stiffeners were successfully produced in ARALL in co-operation with Fokker. Meanwhile some preliminary tests will be carried out on Z-stiffened panels with ARALL skin and aluminium alloy stiffeners.

The preliminary results of the Al-panels shown in the table above, indicate that the program developed is very useful for design work, especially because for these panels the computer time on an AMDAHL computer was only .30 s CPU-time.

The structural efficiencies of the aluminium alloy panels in the table above, together with some calculated ARALL panels, are shown graphically in Figure 16. This figure indicates clearly that the ARALL compression panels are at least equal to the aluminium alloy compression panels.

ARALL IN PRESSURE CABINS

The minimum thickness of the skin of a pressure cabin is generally determined by the fatigue be-

haviour of the material used. It is clear that for this kind of structure ARALL, as a result of its excellent fatigue behaviour, can offer considerable weight savings in comparison with the usual aluminium alloys. To indicate the possible weight saving, the minimum skin thickness of pressure cabins representative of several current aircraft have been recalculated both in aluminium alloy and in ARALL. However, the design criteria for aluminium alloy and ARALL are different. Whereas pressure cabins of Alclad 2024-T3 must be designed on the fatigue behaviour (or crack propagation rate) of the material, the ARALL configuration can be designed on the static properties of the material. At the actual differential pressure p, the allowable stress in the gross cross-sectional area is typically around $\bar{\sigma}$ = 100 MPa for Alclad 2024-T3, for which the joints must be cold-bonded and (countersunk) riveted. Practice has shown that this configuration and stress level give a good fatigue life for the cabin, and this stress level has been used in the subsequent calculations. A second requirement is that no failure may occur at a differential pressure twice the actual pressure. In general it can be said that for the aluminium configuration, the first requirement gives the minimum skin thickness and the second requirement determines the joint geometry.

Due to the excellent fatigue behaviour of ARALL, it is suggested that pressure cabins made of this material can be designed only for this second requirement. From material tests on optimized ARALL, it appears likely that cracks, due to accidental damage or any other cause, will not propagate under any conditions that can be envisaged in a practical pressure cabin made of ARALL (see Figure 8, case R=0).

So, for a useful comparison between the two configurations, it is particularly necessary to consider the joint geometry. In this case only the longitudinal joint is important, because along this joint the load transfer is twice that on the circumferential joint. To achieve a realistic comparison it is considered that the number of rivet rows in the ARALL configuration should not exceed the number of rows in aluminium alloy. This can have the effect of limiting the reduction in thickness with ARALL, because of the loss of rivet strength in thin sheets and the usual restrictions on rivet spacing.

For the calculation of the static strength of the joint the contribution of the bondline will be ignored. This is still a requirement of some Airworthiness Authorities.

However, the question arises whether the usual rived data[14] can be used for ARALL.

Preliminary test results and a tentative analysis of the rivet table have indicated that these data are in fact applicable to ARALL. With the requirements mentioned above, the comparison between the ARALL and aluminium alloy for the pressure cabins of various aircraft is made in the table below. This table shows clearly that weight savings up to 50% are possible. For example, the actual weight saving for the whole cabin would be up to 32500 N for an aircraft such as Boeing 747.

Due to the fact that the factors of safety (FS) given in this table are rivet controlled (both for ARALL and aluminium alloy) while for the ARALL configuration the factors of safety for the skin in the net cross-sectional area are greater than 3.5 and in the gross cross-sectional area in excess of 4.4, it is useful to look for other types of rivets or other forms of connection for the ARALL configuration. The margins of safety are based on the stresses at the actual pressure.

	radius	p	δ_{Al}	SF_{Al}	δ_{ARALL}	SF_{ARALL}	weight saving
Type	mm	MPa	mm	–	mm	–	%
F28	1650	.053	.9	2.27	.8	2.13	23
BAC 1.11	1575	.053	.9	2.38	.8	2.21	23
Boeing 707	1765	.061	1.1	2.77	1.0	2.55	19
Boeing 727	1765	.061	1.1	2.77	1.0	2.55	19
Boeing 747	3240	.063	2.1	2.70	1.3	2.54	48
DC 8	1780	.062	1.1	2.73	1.0	2.51	19
DC 10	3010	.061	1.9	2.89	1.3	2.24	43
A 300B	2820	.058	1.7	2.28	1.3	2.52	36
Lockh. 1011	2885	.062	1.8	2.81	1.3	2.30	40

Potential weight savings on pressure cabins

In the calculation of the strength of the joint, rivet data for countersunk NAS 1097 rivets is used. So it is expected that the allowable load transfer through the joint can be increased by using the newly developed Briles rivet[15]. Use of this rivet may also result in a reduced thickness of the skin and then offers more weight saving. Investigations on this subject are planned.

The weight saving can increase further if wholly bonded joints are used, but only if this type of connection is allowed. So it is necessary to investigate this type of joint, in order to persuade the Airworthiness Authorities of its safety.

DISCUSSION

The data summarized in the previous sections indicate significant improvements in the fatigue properties of ARALL as compared to monolithic aluminium alloys. Especially when a favourable residual stress system is introduced in ARALL, it becomes almost fatigue insensitive. This behaviour can be understood because fibres in the wake of a crack, even for very minute cracks, exert a significant crack opening restraint. In the extreme case crack opening may even be prevented. In other cases the stress-intensity factor K is greatly reduced. This mechanism works only if fibre failure does not occur. It turns out that a certain amount of "self-controlled" delamination occurs between fibres and adhesive, and as a result the fibres in the wake of the crack are not loaded to the point of failure. Further analysis[1] indicates that the load in those fibres will be approximately constant. A theoretical model was developed for calculating K values for a crack in ARALL[16], accounting for the decreasing crack rates as shown in Figure 7.

With regard to static strength in the unnotched and notched condition, ARALL also has better properties than aluminium alloy. The same applies to static strength of riveted and bolted joints.

It thus appears that ARALL is a very attractive material for fatigue critical aircraft components. If fatigue is no longer the decisive design criterion for such components, other critera will emerge. For the wing tension skin of a small transport aircraft this proves to be the buckling strength (negative gust case) while for a pressure cabin skin it is static joint strength in tension. For a stiffened panel loaded in compression the efficiency of ARALL is comparable with aluminium alloy. This follows both from tests and calculations. The spin-off from the analysis was a new calculation method applicable to both isotropic and orthotropic panels, for which a fast computer program was developed for use as a design tool.

For the application of ARALL to fuselage skins, only a theoretical analysis has been made until now. Since the analysis indicates most interesting weight savings further study is certainly worthwhile. The analysis also shows that present airworthiness requirements for classical alloys are not entirely appropriate to ARALL.

CONCLUSIONS

The results of a development program on a new hybrid material for aircraft structural applications has led to the following conclusions:

1. A very promising new hybrid material for aircraft structures can be obtained by the adhesive bonding of a number of thin sheets and thin unidirectional aramid layers. ARALL shows very favourable fatigue crack growth properties and has a high tensile yield strength. This is particularly true if a favourable residual stress system is introduced in the fibre layers and an optimum metal sheet thickness has been chosen. The aluminium alloy sheets are then prestressed in compression.

2. Results of constant-amplitude tests and flight-simulation fatigue tests on lugs, centrally cracked specimens bolted and riveted joint specimens show highly superior fatigue properties in all cases for ARALL, as compared with monolithic aluminium alloy. An almost fatigue insensitive behaviour of ARALL was found. Cracks initiating from open holes were arrested after a small amount of crack growth (2 - 3 mm) under extremely severe flight simulation loading. The fatigue behaviour was also excellent in a corrosive environment, while no effect of precorrosion was found.

3. With respect to static strength in the unnotched and notched condition, ARALL also has better properties than aluminium alloy.

4. In spite of the use of structural fibres in the laminate, nearby all the advantages of metals over pure composites are preserved, such as: plasticity, impact strength, lightning resistance, high specific isotropic stiffness, formability and easy machining. The material can easily be cut, drilled, sawn and milled. Joining by bolting and riveting is possible. (Curing and prestressing of ARALL does not require new technologies.) So conventional metal working and metal bonding techniques may be used in assembling aircraft components using the new material. For certain applications plastic sheet bending is possible, including the fabrication of stiffeners.

5. As a result of this information it appears that ARALL is a promising material for structural applications, especially where fatigue is a significant design criterion in setting allowable stress levels. Calculations for a preliminary design on a wing tension skin and on fuselage skins of different types of aircraft indicate a weight saving for the wing skin of more than 30 percent and for the fuselage skins from 20 to 50 percent.

6. In view of the buckling strength of ARALL panels a new calculation method (OBSOZPAN) was developed for both isotropic and orthotropic material. Because it is a very fast calculation program it can be used as a design tool.

REFERENCES

1. Vogelesang, L.B.; Marissen, R. and Schijve, J.: "A New Fatigue Resistant Material: Aramid Reinforced Aluminium Laminate (ARALL)", paper presented at the 11th I.C.A.F. Symposium, May 1981, Noordwijkerhout, The Netherlands. Also Report LR-322, Delft University of Technology, Department of Aerospace Engineering, 1981.

2. Oken, S. and June, R.R.: "Analytical and Experimental Investigation of Aircraft Metal Structures Reinforced with Filamentary Composites", NASA CR-1859, December 1971.

3. Hengel, C.G. van: "A Simple Method to Calculate the Static Properties of Unnotched ARALL" (in Dutch), Thesis, Delft University of Technology, Department of Aerospace Engineering, March 1982.

4. Schee, P.A. van der: "Outerwing Lowerskin Fatigue Testing as a Part of the Continuing Airworthiness Programme of the Fokker F27", paper presented at the 10th I.C.A.F. Symposium, Brussel, May 1979.

5. Heijdra, J.J. and Venselaar, C.F.: "An ARALL Lower Wing Skin for the Fokker F27 Friendship" (in Dutch), Thesis, Delft University of Technology, Department of Aerospace Engineering, April 1981.

6. Wanhill, R.J.H.; Luccia, J.J. de and Vogelesang, L.B.: "Environmental Fatigue of Aluminium Alloy Structural Joints", paper prepared for the 7th International Light Metals Congress, Leoben-Vienna, June 1981.

7. Warnar, F.W.: "Symmetric and Nonsymmetric ARALL Butt Strap Joints" (in Dutch), Document B2-82-07, Delft University of Technology, Department of Aerospace Engineering, March 1982.

8. Schijve, J.; Jacobs, F.A. and Meulman, A.E.: "Effect of an Anti-Corrosion Penetrant on the Fatigue Life in Flight-Simulation Tests on Various Riveted Joints", NLR Report TR 77103 U, Amsterdam 1977.

9. "Metallic Materials and Elements for Aerospace Vehicle Structures", Mil-HdBk-5A, Department of Defense, Washington D.C., 1966.

10. Neut, A. van der: "Overall Buckling of Z-stiffened Panels in Compression", Report LR-303, Delft University of Technology, Department of Aerospace Engineering, August 1980.

11. Gunnink, J.W.: "Overall Buckling of Specially Orthotropic Z-stiffened Panels. Part I: Theory", Report LR-351, Delft University of Technology, Department of Aerospace Engineering, April 1982.

12. Gunnink, J.W.: "Overall Buckling of Specially Orthotropic Z-stiffened Panels. Part II, Computer Program", to be published.

13. Sloot, J.H. van der: "Recent Advances with the 'Experimental Method Fokker (EMF)' to Predict Critical Loads of Stringer-Stiffened Panels", ICAS-80-20.1, 12th Congress International Council of the Aeronautical Sciences, October 1980.

14. "Fokker Technical Handbook, Part 3, Strenght Data".

15. "Fast Rivet Catalog", Briles Rivet Corporation.

16. Marissen, R. and Vogelesang, L.B.: "Development of a New Hybrid Material: ARALL", paper presented at the Intercontinental SAMPE meeting, Cannes, France, January 1981.

17. Williams, J.G. and Mikulas, M.M. Jr.: "Analytical and Experimental Study of Structural Efficient Composite Hat-stiffened Panels Loaded in Axial Compression", AIAA paper No. 75-754, AIAA/ASME/SAE 16th Structures, Structural Dynamics, and Materials Conference, Denver, Colorado, May 1975.

18. Hartman, A.: "Fatigue Tests on Single Lap Joints in Clad 2024-T3 Aluminium Alloy Manufactured by a Combination of Riveting and Adhesive Bonding", National Aerospace Laboratory NLR, Report M-2170, 1966.
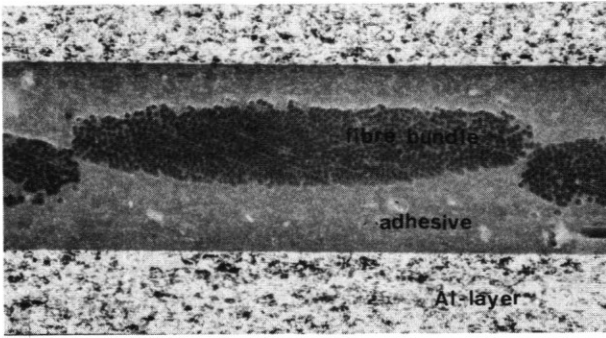
magnification 85 x

Figure 1   Cross-section of ARALL sheet specimen
           (Type A)
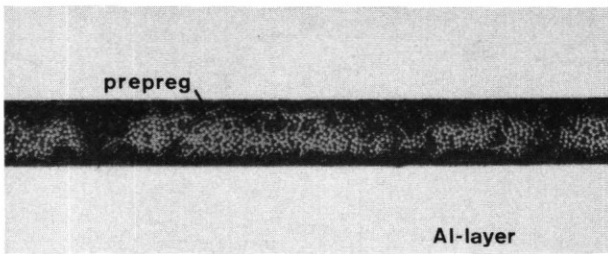
magnification 50 x

Figure 3   Cross-section of ARALL sheet specimen
           (Type B)
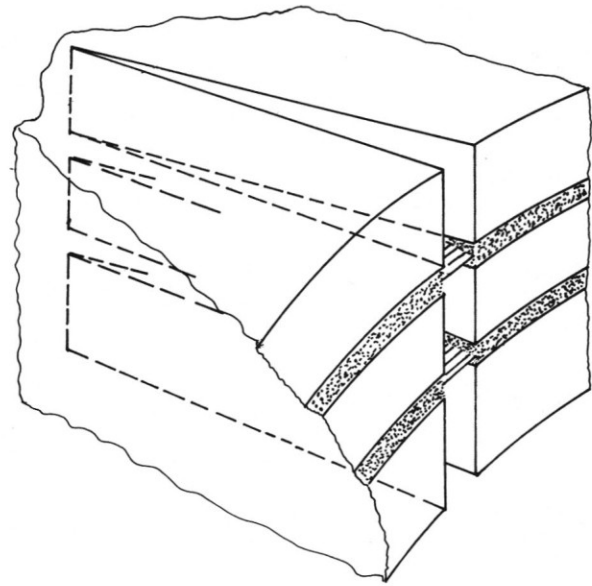

Figure 2   Fatigue crack in ARALL.
           The ARALL material is optimized in a way
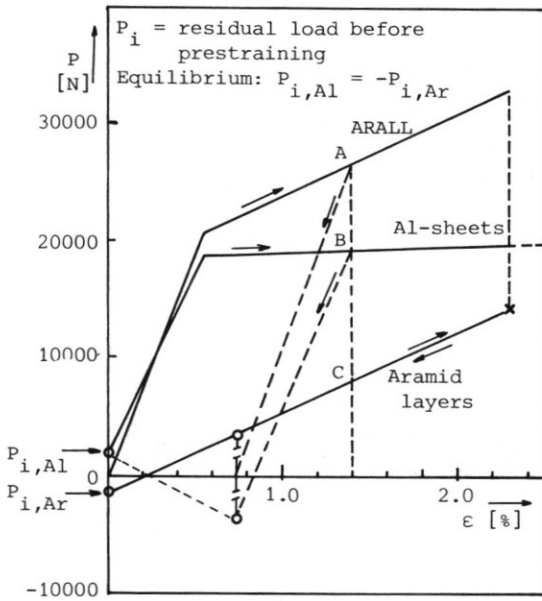   no fibre failure will happen

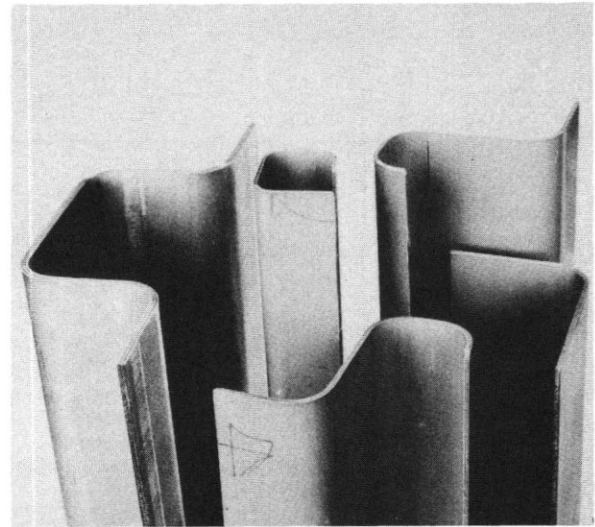Figure 4   Load-strain curve of ARALL sheet specimen
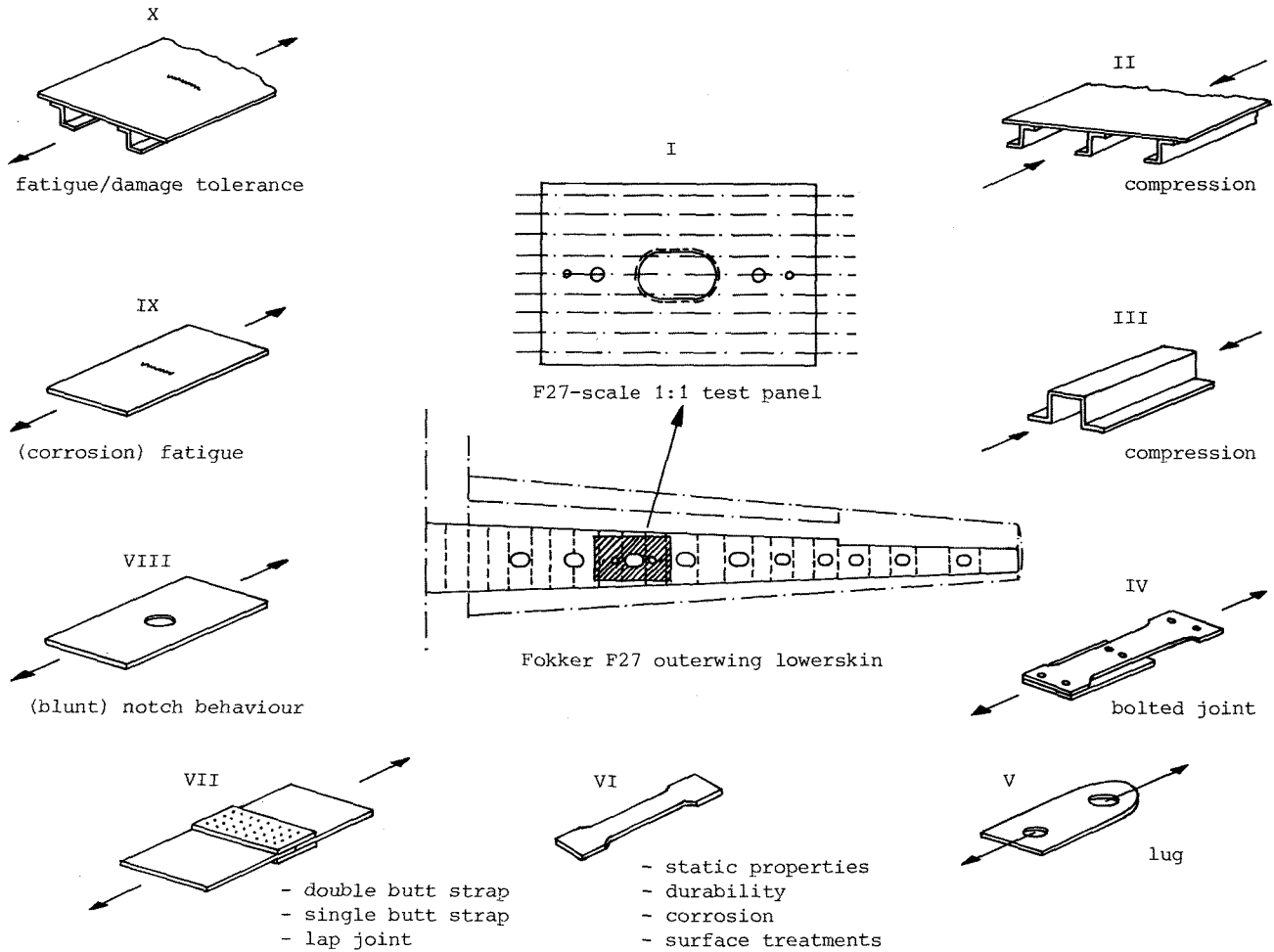

Figure 5   Some ARALL products

X

fatigue/damage tolerance

IX

(corrosion) fatigue

VIII

(blunt) notch behaviour

VII
- double butt strap
- single butt strap
- lap joint

I

F27-scale 1:1 test panel

Fokker F27 outerwing lowerskin

VI
- static properties
- durability
- corrosion
- surface treatments

II

compression

III

compression

IV

bolted joint

V

lug

Figure 6   The structural development program for a transport aircraft wing
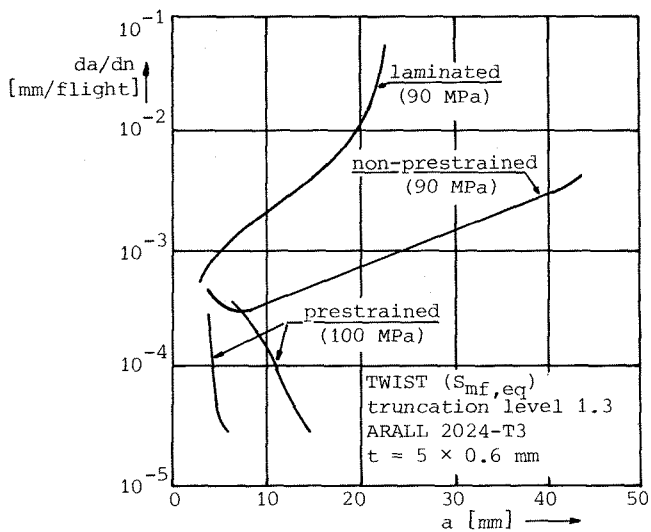
Figure 7   Crack-propagation rates in 2024-T3
laminated material and ARALL
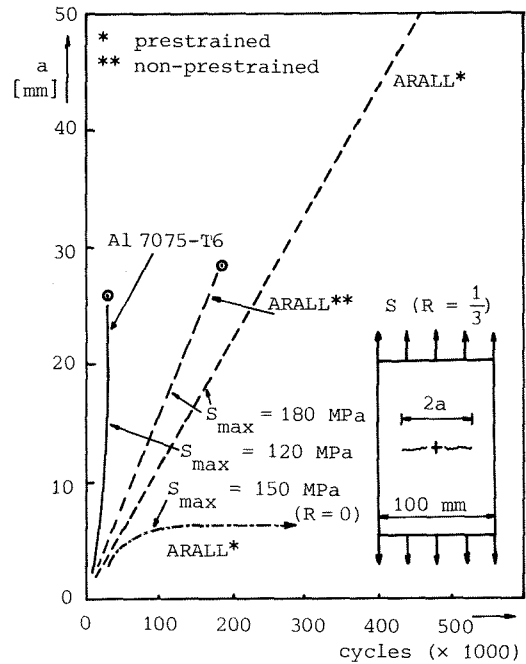
Figure 8   Crack-propagation lives until failure
under constant-amplitude loading

998
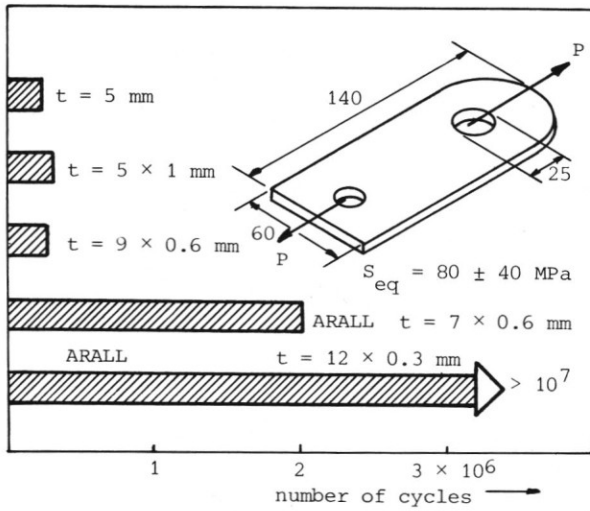
Figure 9 Comparison of fatigue lives. Results of constant-amplitude tests on lugs. Material: 2024-T3, laminated and ARALL (no prestrain, no prestress)
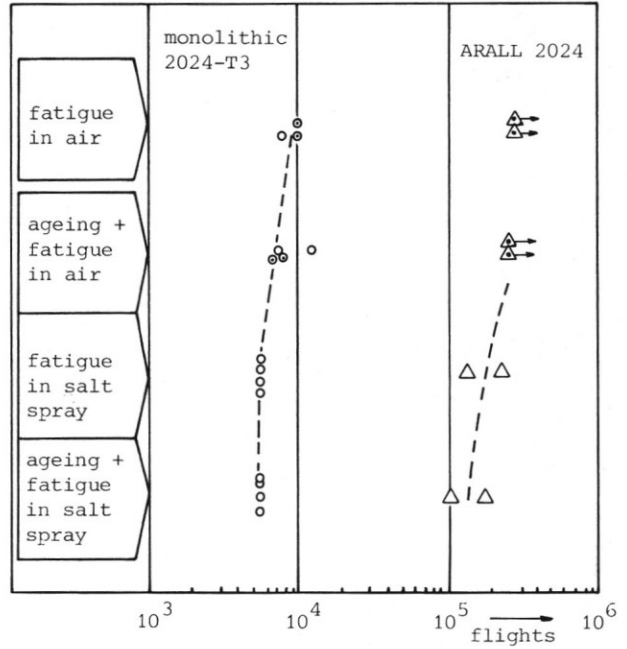
Figure 10 Fatigue lives until failure of bolted joint specimens under Mini TWIST gust spectrum with S_{mf} = 101 MPa
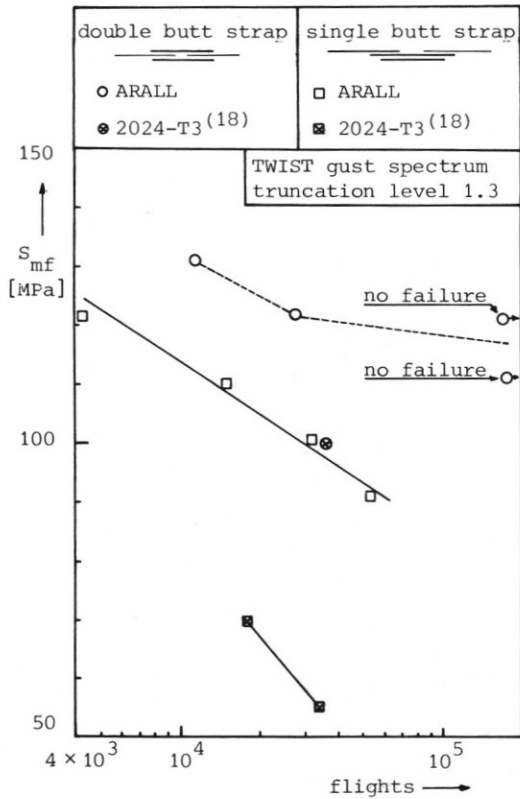
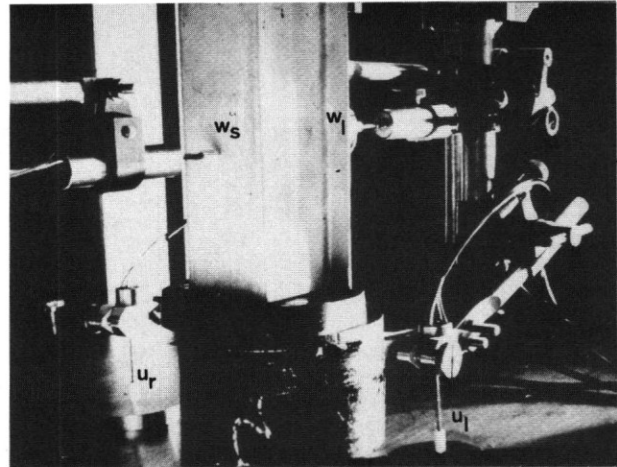Figure 11 Fatigue lives until failure of single and double butt strap bolted joints

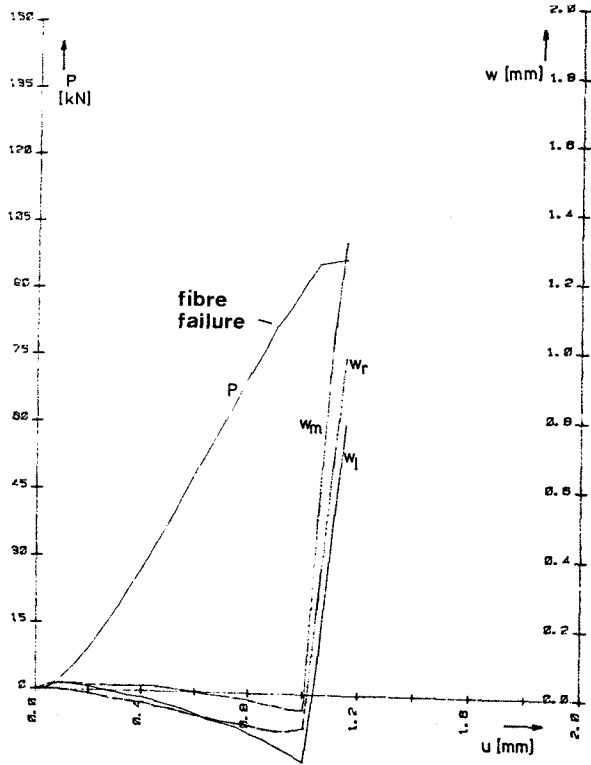Figure 12 Local buckling, test specimen in the 800 kN compression machine

Figure 13 Load-shortening and out-of-plane displacement shortening curve of test specimen ARALL 1
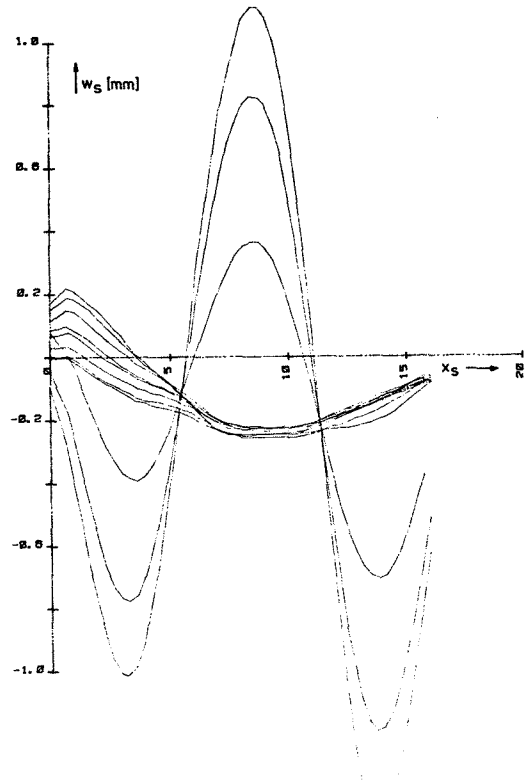

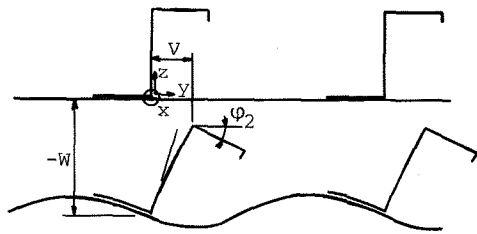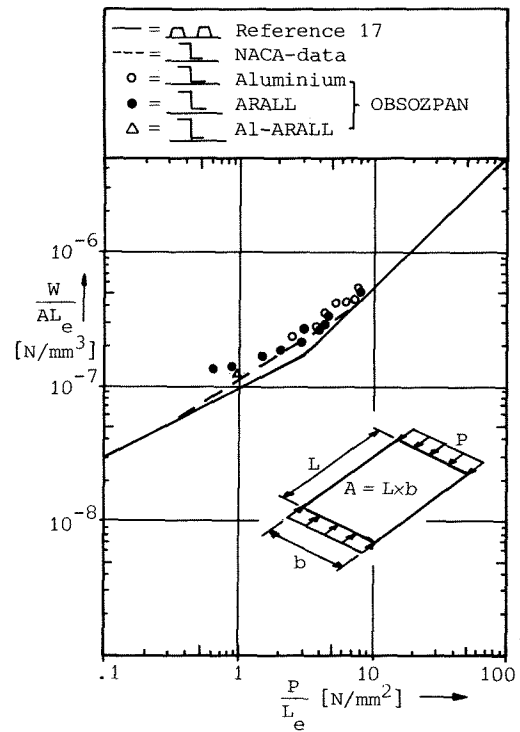Figure 14 Buckle pattern of test specimen ARALL 1

Figure 15 Overall flange buckling

Figure 16 Structural efficiency of Z-stiffened panels